mathematics

MDPI

Article

A Numerical Algorithm for the Solutions of ABC Singular Lane–Emden Type Models Arising in Astrophysics Using Reproducing Kernel Discretization Method

Omar Abu Arqub [1], Mohamed S. Osman [2,3,*], Abdel-Haleem Abdel-Aty [4,5], Abdel-Baset A. Mohamed [6,7] and Shaher Momani [8,9]

1 Department of Mathematics, Faculty of Science, Al-Balqa Applied University, Salt 19117, Jordan; o.abuarqub@bau.edu.jo
2 Department of Mathematics, Faculty of Science, Cairo University, Giza 12613, Egypt
3 Department of Mathematics, Faculty of Applied Science, Umm Alqura University, Makkah 21955, Saudi Arabia
4 Department of Physics, College of Sciences, University of Bisha, P.O. Box 344, Bisha 61922, Saudi Arabia; amabdelaty@ub.edu.sa
5 Physics Department, Faculty of Science, Al-Azhar University, Assiut 71524, Egypt
6 Department of Mathematics, College of Science and Humanities in Al-Aflaj, Prince Sattam bin Abdulaziz University, Al-Aflaj 11942, Saudi Arabia; a.mohamed@psau.edu.sa
7 Faculty of Science, Assiut University, Assiut 71515, Egypt
8 Department of Mathematics and Sciences, College of Humanities and Sciences, Ajman University, Ajman, UAE; s.momani@ju.edu.jo
9 Department of Mathematics, Faculty of Science, The University of Jordan, Amman 11942, Jordan
* Correspondence: mofatzi@sci.cu.edu.eg; Tel.: +20-1005724357

Received: 6 May 2020; Accepted: 3 June 2020; Published: 5 June 2020

check for updates

Abstract: This paper deals with the numerical solutions and convergence analysis for general singular Lane–Emden type models of fractional order, with appropriate constraint initial conditions. A modified reproducing kernel discretization technique is used for dealing with the fractional Atangana–Baleanu–Caputo operator. In this tendency, novel operational algorithms are built and discussed for covering such singular models in spite of the operator optimality used. Several numerical applications using the well-known fractional Lane–Emden type models are examined, to expound the feasibility and suitability of the approach. From a numerical viewpoint, the obtained results indicate that the method is intelligent and has several features stability for dealing with many fractional models emerging in physics and mathematics, using the new presented derivative.

Keywords: Atangana–Baleanu–Caputo fractional derivative; fractional Lane–Emden type models; reproducing kernel discretization method

1. Prolegomena and Presentation

Fractional calculus is dealing with investigations and applications of derivatives and integrations of arbitrary order that provide an attractive mechanism for explaining the memory and hereditary effort of complex systems [1–5]. Fractional calculus theory dates back to Leibniz in the sixteenth century, and after that, many forms of fractional operators have been introduced in the classical theory. Among them are the Riemann–Liouville, Caputo–Liouville, Atangana–Baleanu–Caputo, and Riesz operator approaches [6–18]. Fractional calculus attracted focus in current scientific research, due to its nonlocal nature and its ability to handle the effects of external forces of phenomena that cannot be modeled in a traditional way. Recently, a new definition of fractional derivative has proposed, the ABC fractional derivative [19–31].

At all events, it is not easy to find accurate numerical solutions to FLETM due to the complexity that occurs inside the Mittag–Leffler function in the fractional ABC derivatives. Thereafter, software computer programming is ordinarily used to obtain numerical solutions in acceptable accuracy. Over this treatise, we face to utilize the RKDM to gain approximate numerical outcomes of FLETM, utilizing the ABC fractional sense. More specifically, we consider the subsequent form [32,33].

$$ {}_{0}^{ABC}\partial_{l}^{\delta}\psi(l)+\frac{\kappa_1}{q_1(l)}\partial_{l}\psi(l)+\frac{\kappa_2}{q_2(l)}\psi(l)+\Phi(l,\psi(l))=\mathrm{T}(l), \tag{1} $$

subject to the CICs

$$ \psi(0)=\alpha \text{ and } \partial_{l}\psi(0)=\beta. \tag{2} $$

We are standing for the following: $l\in\mathcal{J}[0,1]$; $\delta\in(1,2]$; $\alpha,\beta,\kappa_1,\kappa_2\in\mathbb{R}$ with $\kappa_1\neq 0\neq\kappa_2$; $\psi\in C(\mathcal{J}\to\mathbb{R})$; $q_1,q_2\in C(\mathcal{J}\to\mathbb{R})$ while $q_1(0)=0=q_2(0)$; $\Phi\in C(\mathcal{J}\times\mathbb{R}\to\mathbb{R})$; $\mathrm{T}\in C(\mathcal{J}-\{0\}\to\mathbb{R})$. We are recording ${}_{0}^{ABC}\partial_{l}^{\delta}\psi(l)$ to sign the ABC fractional derivative of ψ in l over $\mathcal{J}$ of order δ with

$$ {}_{0}^{ABC}\partial_{l}^{\delta}\psi(l)=(1-\delta)\left(1-\delta+\delta\Gamma^{-1}(\delta)\right)\int_{0}^{l}\partial^{2}\psi(k)\sum_{n=0}^{\infty}\frac{(-1)^{n}}{\Gamma(n\delta+1)}\left(\frac{\delta}{2-\delta}\right)^{n}(l-k)^{n\delta}dk, \tag{3} $$

in which $l=0$ is a base point acquaint at $l\in\mathcal{J}-\mathfrak{B}(\mathcal{J})$ and $\psi\in\mathcal{S}^{2}(\mathcal{J}-\mathfrak{B}(\mathcal{J}))$, whereas $\mathcal{S}^{2}$ is the Sobolev functions' space of order 2 on the domain $\mathcal{J}$ except the boundary $\mathfrak{B}(\mathcal{J})$ of $\mathcal{J}$ erected as

$$ \mathcal{S}^{2}(\mathcal{J}-\mathfrak{B}(\mathcal{J}))=\left\{\psi\in L^{2}(\mathcal{J}-\mathfrak{B}(\mathcal{J})):\partial_{l}\psi(l),\partial_{l}^{2}\psi(l)\in L^{2}(\mathcal{J}-\mathfrak{B}(\mathcal{J}))\right\}. \tag{4} $$

The FLETM is categorized as a singular differential problem and supplied as an instrument in the formulation of the phenomena that emerge with various applications across mathematical physics and astrophysics. It characterizes the equilibrium thickness allocation in the self-gravitating sphere of polytrophic isothermal gas and, at the origin, contained singularity nodes. The FLETM has weight in the domain of modeling the clusters of galaxies, stellar structure, and radiative cooling. Interested reader can go through [32–36], to identify more details, properties, results, and applications on such singular models.

The standard RKDM main field topics are in the modelling and simulation of sundry-dimensional issues in applied computational physical, applied mathematics, and engineering [37–39], it has been used in creating numerical and approximate solutions for integral and differential models in the shape of infinite convergent series with floor extent of calculations, without any limited assumptions. This approach adjusted has been utilized as a solver technique to deal with complexes' nonlinear and discontinues shapes of integral/differential problems arising in various applications area range from engineering to physics as utilized in [40–59].

2. Concrete Structure of the RKDM

This part is dedicated to describing some adaptive necessary rules and preliminaries for the RKDM, especially those concerning the kernel functions and independency. We take $AC(\mathcal{J})$ to denote the set of absolutely continuous functions on $\mathcal{J}$ and we take $L^{2}(\mathcal{J})$ to denote the set of square-integrable functions on $\mathcal{J}$.

Assume that $\mathbb{H}$ is a reproducing kernel Hilbert space. From the Riesz representation theorem, it follows that for every $k\in\mathcal{J}$, there exists only one $H_{l}(k)\in\mathbb{H}$, such that for every $F\in\mathbb{H}$, we have

$$ \forall k\in\mathcal{J}:\ \langle F(k),H_{l}(k)\rangle_{\mathbb{H}}=F(l). \tag{5} $$

Definition 1. *[23] Let $\Pi(\mathcal{J})$ be a Hilbert space with inner product and functional structures, as is given below:*

$$\begin{cases} \Pi(\mathcal{J}) = \left\{\psi(l) : \psi(l), \partial_l \psi(l), \partial_l^2 \psi(l) \in AC(\mathcal{J});\ \partial_l^3 \psi(l) \in L^2(\mathcal{J}); \psi(0) = \partial_l \psi(0) = 0\right\}, \\ \langle \psi_1(l), \psi_2(l) \rangle_\Pi = \partial_l^2 \psi_1(0) \partial_l^2 \psi_2(0) + \int_{\mathcal{J}} \partial_l^3 \psi_1(l) \partial_l^3 \psi_2(l) dl, \\ \|\psi\|_\Pi = \sqrt{\psi(l), \psi(l)_\Pi}. \end{cases} \tag{6}$$

Definition 2. *[23] Let $\Delta(\mathcal{J})$ be a Hilbert space with inner product and functional structures, as is given below:*

$$\begin{cases} \Delta(\mathcal{J}) = \left\{\psi(l) : \psi(l) \in AC(\mathcal{J});\ \partial_l \psi(l) \in L^2(\mathcal{J})\right\}, \\ \langle \psi_1(l), \psi_2(l) \rangle_\Delta = \int_{\mathcal{J}} \psi_1(l) \psi_2(l) dl + \partial_l \psi_1(l) \partial_l \psi_2(l) dl, \\ \|\psi\|_\Delta = \sqrt{\psi(l), \psi(l)_\Delta}. \end{cases} \tag{7}$$

Theorem 1. *[23] The space $\Pi(\mathcal{J})$ is a complete reproducing kernel with rule*

$$F_l(k) = \frac{1}{120} \begin{cases} l^2\left(-5k^2 l + k^3 + 10 l^2 (3 + k)\right), k \le l, \\ k^2\left(-5 l^2 k + l^3 + 10 k^2 (3 + l)\right), k > l. \end{cases} \tag{8}$$

Theorem 2. *[23] The space $\Delta(\mathcal{J})$ is a complete reproducing kernel with rule*

$$G_l(k) = \frac{sinh(1)}{2} \begin{cases} cosh(l + k - 1) + cosh(l - k - 1), k \le l, \\ cosh(l + k - 1) + cosh(k - l - 1), k > l. \end{cases} \tag{9}$$

When applied the RKDM, one must firstly split the convex compact set $\mathcal{J}$ into regular sections encoded with l_i. This assumes that the acquired set $\{l_i\}_{i=1}^{\infty}$ will be dense in $\mathcal{J}$. We attempt to cover $\mathcal{J}$, as well as the numerical procedure ought to end in finite phases.

To examine the independency, suppose $\{\theta_i\}_{i=1}^{m}$ are not all zero, such that $\sum_{i=1}^{m} \theta_i F_{l_i}(k) = 0$. Take $h_s(k) \in \Pi(\mathcal{J})$, such that $h_s(k_i) = \delta_{i,k}$, $\forall i = 1, 2, \ldots, m$, then

$$\begin{aligned} 0 = & \left\langle h_s(k), \sum_{i=1}^{m} \theta_i F_{l_i}(k) \right\rangle_\Pi \\ & = \sum_{i=1}^{m} \theta_i h_s(k), F_{l_i}(k)_\Pi \\ & = \sum_{i=1}^{m} \theta_i h_s(k_i) \\ & = \theta_i, \end{aligned} \tag{10}$$

for $i = 1, 2, \ldots, m$. This shows that $\left\{F_{l_i}(k)\right\}_{i=1}^{m}$ is linearly independent for all $m \ge 1$ and, thus, $\left\{F_{l_i}(k)\right\}_{i=1}^{\infty}$ is linearly independent in $\Pi(\mathcal{J})$. Similarly, one can find that $\left\{G_{l_i}(k)\right\}_{i=1}^{\infty}$ is linearly independent too.

3. Solutions Shape of FLETM

Multiplying (1) by $q_1(l) q_2(l)$, we get

$$q(l) {}_0^{ABC}\partial_l^\delta \psi(l) + \kappa_1 q_2(l) \partial_l \psi(l) + \kappa_2 q_1(l) \psi(l) + \overline{\Phi}(l, \psi(l)) = \overline{\mathrm{T}}(l), \tag{11}$$

in which $q(l) = q_1(l) q_2(l)$, $\overline{\Phi}(l, \psi(l)) = q_1(l) q_2(l) \Phi(l, \psi(l))$, and $\overline{\mathrm{T}}(l) = q_1(l) q_2(l) \mathrm{T}(l)$.

The replacement $\psi(l) :\to \psi(l) - (\beta l + \alpha)$ converts FLETM given by (11) and (2) into homogenous one. We are denoting the new equation by

$$q(l) {}_0^{ABC}\partial_l^\delta \psi(l) + \kappa_1 q_2(l) \partial_l \psi(l) + \kappa_2 q_1(l) \psi(l) + \overline{\Phi}(l, \psi(l) - (\beta l + \alpha)) = \overline{\overline{\mathrm{T}}}(l), \tag{12}$$

subject to the CICs

$$\psi(0) = 0 \text{ and } \partial_l \psi(0) = 0. \tag{13}$$

The function $\overline{\overline{\mathrm{T}}}(l)$ appears from substituting $\psi(l) - (\beta l + \alpha)$ instead of $\psi(l)$ in (12). In fact, after simplification and transform the extra mathematical terms into the right hand side of (12), one can write $\overline{\overline{\mathrm{T}}}(l) = q(l)^{ABC}_{0}\partial^{\delta}_{l}(\beta l + \alpha) + \kappa_1 q_2(l)\partial_l(\beta l + \alpha) + \kappa_2 q_1(l)(\beta l + \alpha) + \overline{\mathrm{T}}(l)$.

Define the linear operator $\mathcal{A} : \Pi(\mathcal{J}) \to \Delta(\mathcal{J})$ and its map $\mathcal{A}[\psi](l)$ as

$$\mathcal{A}[\psi](l) = q(l)^{ABC}_{0}\partial^{\delta}_{l}\psi(l) + \kappa_1 q_2(l)\partial_l \psi(l) + \kappa_2 q_1(l)\psi(l). \tag{14}$$

Putting $\zeta(l, \psi(l), \partial_l \psi(l)) := \overline{\overline{\mathrm{T}}}(l) - \overline{\Phi}(l, \psi(l) - (\beta l + \alpha))$, then (14) and (13) are converted into the form

$$\begin{cases} \mathcal{A}[\psi](l) = \zeta(l, \psi(l), \partial_l \psi(l)), \\ \psi(0) = 0 \textit{ and } \partial_l \psi(0) = 0. \end{cases} \tag{15}$$

We arrange the system of orthogonal functions taking $\mathfrak{S}_i(l) = G_{l_i}(l)$, $\Lambda_i(l) = \mathcal{A}^*[\mathfrak{S}_i](l)$, $i = 1, 2, 3, \ldots$, such that $\{l_i\}_{i=1}^{\infty}$ is dense on $\mathcal{J}$. The Gram–Schmidt orthogonalization process is used to generate the system of orthonormal functions $\left\{ \overline{\Lambda}_i(l) \right\}_{i=1}^{\infty}$ on $\Pi(\mathcal{J})$, where

$$\overline{\Lambda}_i(l) = \sum_{j=1}^{i} \varepsilon_{ij} \Lambda_j(l), \tag{16}$$

with the orthogonalization coefficients ε_{ij} with the indexes $i = 2, 3, \ldots$, and $j = 1, 2, \ldots, i-1$ are computed in the subsequent algorithm.

Algorithm 1. Steps of the orthonormal Gram–Schmidt process:

Step 1: For $i = 2, 3, \ldots$ and $j = 1, 2, \ldots, i-1$, do the following:

$$\begin{aligned} \varepsilon_{11} &= \tfrac{1}{\|\Lambda_1\|_{\Pi}}, \\ \varepsilon_{ii} &= \frac{1}{\sqrt{\|\Lambda_i\|^2_{\Pi} - \sum_{p=1}^{i-1} \langle \Lambda_i(t), \overline{\Lambda}_p(t) \rangle^2_{\Pi}}}, i \neq 1, \\ \varepsilon_{ij} &= -\frac{1}{\sqrt{\|\Lambda_i\|^2_{\Pi} - \sum_{p=1}^{i-1} \langle \Lambda_i(t), \overline{\Lambda}_p(t) \rangle^2_{\Pi}}} \sum_{p=j}^{i-1} \langle \Lambda_i(t), \overline{\Lambda}_p(t) \rangle_{\Pi} \varepsilon_{pj}, i > j. \end{aligned} \tag{17}$$

Output: The orthogonalization coefficients ε_{ij}.

Step 2: For $i = 1, 2, 3, \ldots$ set

$$\overline{\Lambda}_i(l) = \sum_{j=1}^{i} \varepsilon_{ij} \Lambda_j(l). \tag{18}$$

Output: System of orthonormal functions $\left\{ \overline{\Lambda}_i(l) \right\}_{i=1}^{\infty}$.

Remark 1. *In the third formula of (17), the calculations of ε_{ij}, $i > j$ are obtaining recursively as follows:*

- *If $i = 2$ and $j = 1$*, then

$$\varepsilon_{21} = -\frac{1}{\sqrt{\|\Lambda_2\|^2_{\Pi} - \sum_{p=1}^{1} \langle \Lambda_1(t), \overline{\Lambda}_p(t) \rangle^2_{\Pi}}} \sum_{p=1}^{1} \langle \Lambda_2(t), \overline{\Lambda}_p(t) \rangle_{\Pi} \varepsilon_{p1}, \tag{19}$$

where

$$\begin{aligned} \sum_{p=1}^{1} \langle \Lambda_2(t), \overline{\Lambda}_p(t) \rangle_{\Pi} \varepsilon_{p1} &= \langle \Lambda_2(t), \overline{\Lambda}_1(t) \rangle_{\Pi} \varepsilon_{11} \\ &= \langle \Lambda_2(t), \overline{\Lambda}_1(t) \rangle_{\Pi} \tfrac{1}{\|\Lambda_1\|_{\Pi}}. \end{aligned} \tag{20}$$

- *If $i = 3$ and $j = 1, 2$, then*

$$\varepsilon_{31} = -\frac{1}{\sqrt{\|\Lambda_3\|_\Pi^2 - \sum_{p=1}^{2}\langle \Lambda_3(t), \overline{\Lambda}_p(t)\rangle_\Pi^2}} \sum_{p=1}^{2} \langle \Lambda_3(t), \overline{\Lambda}_p(t)\rangle_\Pi \varepsilon_{p1}, \tag{21}$$

where

$$\begin{aligned} \sum_{p=1}^{2} \langle \Lambda_3(t), \overline{\Lambda}_p(t)\rangle_\Pi \varepsilon_{p1} &= \langle \Lambda_3(t), \overline{\Lambda}_1(t)\rangle_\Pi \varepsilon_{11} + \langle \Lambda_3(t), \overline{\Lambda}_2(t)\rangle_\Pi \varepsilon_{21} \\ &= \langle \Lambda_3(t), \overline{\Lambda}_1(t)\rangle_\Pi \frac{1}{\|\Lambda_1\|_\Pi} + \langle \Lambda_3(t), \overline{\Lambda}_2(t)\rangle_\Pi \varepsilon_{21} \end{aligned} \tag{22}$$

in which ε_{21} comes from (19). Similarly,

$$\varepsilon_{32} = -\frac{1}{\sqrt{\|\Lambda_3\|_\Pi^2 - \sum_{p=1}^{2}\langle \Lambda_3(t), \overline{\Lambda}_p(t)\rangle_\Pi^2}} \sum_{p=2}^{2} \langle \Lambda_3(t), \overline{\Lambda}_p(t)\rangle_\Pi \varepsilon_{p2}, \tag{23}$$

where

$$\begin{aligned} \sum_{p=2}^{2} \langle \Lambda_3(t), \overline{\Lambda}_p(t)\rangle_\Pi \varepsilon_{p2} &= \langle \Lambda_3(t), \overline{\Lambda}_2(t)\rangle_\Pi \varepsilon_{22} \\ &= \langle \Lambda_3(t), \overline{\Lambda}_2(t)\rangle_\Pi \frac{1}{\sqrt{\|\Lambda_2\|_\Pi^2 - \sum_{p=1}^{1}\langle \Lambda_2(t), \overline{\Lambda}_p(t)\rangle_\Pi^2}}. \end{aligned} \tag{24}$$

- *If $i = 4$ and $j = 1, 2, 3$ then*

$$\varepsilon_{41} = -\frac{1}{\sqrt{\|\Lambda_4\|_\Pi^2 - \sum_{p=1}^{3}\langle \Lambda_4(t), \overline{\Lambda}_p(t)\rangle_\Pi^2}} \sum_{p=1}^{3} \langle \Lambda_4(t), \overline{\Lambda}_p(t)\rangle_\Pi \varepsilon_{p1}, \tag{25}$$

where

$$\begin{aligned} \sum_{p=1}^{3} \langle \Lambda_4(t), \overline{\Lambda}_p(t)\rangle_\Pi \varepsilon_{p1} &= \langle \Lambda_4(t), \overline{\Lambda}_1(t)\rangle_\Pi \varepsilon_{11} + \langle \Lambda_4(t), \overline{\Lambda}_2(t)\rangle_\Pi \varepsilon_{21} + \langle \Lambda_4(t), \overline{\Lambda}_3(t)\rangle_\Pi \varepsilon_{31} \\ &= \langle \Lambda_4(t), \overline{\Lambda}_1(t)\rangle_\Pi \frac{1}{\|\Lambda_1\|_\Pi} + \langle \Lambda_4(t), \overline{\Lambda}_2(t)\rangle_\Pi \varepsilon_{21} + \langle \Lambda_4(t), \overline{\Lambda}_3(t)\rangle_\Pi \varepsilon_{31}, \end{aligned} \tag{26}$$

in which ε_{21} comes from (19) and ε_{31} comes from (21). Similarly,

$$\varepsilon_{42} = -\frac{1}{\sqrt{\|\Lambda_4\|_\Pi^2 - \sum_{p=1}^{3}\langle \Lambda_4(t), \overline{\Lambda}_p(t)\rangle_\Pi^2}} \sum_{p=2}^{3} \langle \Lambda_4(t), \overline{\Lambda}_p(t)\rangle_\Pi \varepsilon_{p2}, \tag{27}$$

where

$$\begin{aligned} \sum_{p=2}^{3} \langle \Lambda_4(t), \overline{\Lambda}_p(t)\rangle_\Pi \varepsilon_{p2} &= \langle \Lambda_4(t), \overline{\Lambda}_2(t)\rangle_\Pi \varepsilon_{22} + \langle \Lambda_4(t), \overline{\Lambda}_3(t)\rangle_\Pi \varepsilon_{32} \\ &= \langle \Lambda_4(t), \overline{\Lambda}_2(t)\rangle_\Pi \frac{1}{\sqrt{\|\Lambda_i\|_\Pi^2 - \sum_{p=1}^{i-1}\langle \Lambda_i(t), \overline{\Lambda}_p(t)\rangle_\Pi^2}} + \langle \Lambda_4(t), \overline{\Lambda}_3(t)\rangle_\Pi \varepsilon_{32}, \end{aligned} \tag{28}$$

in which ε_{32} comes from (23). Finally,

$$\varepsilon_{43} = -\frac{1}{\sqrt{\|\Lambda_4\|_\Pi^2 - \sum_{p=1}^{3}\langle \Lambda_4(t), \overline{\Lambda}_p(t)\rangle_\Pi^2}} \sum_{p=3}^{3} \langle \Lambda_4(t), \overline{\Lambda}_p(t)\rangle_\Pi \varepsilon_{p3}, \tag{29}$$

where

$$\begin{aligned}\sum_{p=3}^{3}\langle\Lambda_4(t),\overline{\Lambda}_p(t)\rangle_{\Pi}\varepsilon_{p3} &= \langle\Lambda_4(t),\overline{\Lambda}_3(t)\rangle_{\Pi}\varepsilon_{33}\\ &= \langle\Lambda_4(t),\overline{\Lambda}_3(t)\rangle_{\Pi}\frac{1}{\sqrt{\|\Lambda_3\|_{\Pi}^2-\sum_{p=1}^{2}\langle\Lambda_3(t),\overline{\Lambda}_p(t)\rangle_{\Pi}^2}}.\end{aligned} \tag{30}$$

Analogue for the remaining indexes $i = 4,\ 5,\dots$ and $j = 1,2,\dots,i-1$.

Lemma 1. *The system$\{\Lambda_i(l)\}_{i=1}^{\infty}$ is complete on $\Pi(\mathcal{J})$.*

Proof. $\Lambda_i(l) = \mathcal{A}^*[\mathfrak{S}_i](l)$ assures that $\Lambda_i(l) \in \Pi(\mathcal{J})$. For each $\psi(l) \in \Pi(\mathcal{J})$, if $\langle\psi(l),\Lambda_i(l)\rangle_{\Pi} = 0$, $i = 1,2,\dots$, then

$$\begin{aligned}\langle\psi(l),\Lambda_i(l)\rangle_{\Pi} &= \langle\psi(l),\mathcal{A}^*[\mathfrak{S}_i](l)\rangle_{\Pi}\\ &= \langle\mathcal{A}[\psi](l),\mathfrak{S}_i(l)\rangle_{\Delta}\\ &= \mathcal{A}[\psi](l_i)\\ &= 0.\end{aligned} \tag{31}$$

From (5) we get $\mathcal{A}[\psi](l_i) = \langle\mathcal{A}[\psi](l),\mathfrak{S}_i(l)\rangle_{\Pi} = 0$. By the density of $\{l_i\}_{i=1}^{\infty}$ in $\mathcal{J}$, we have $\mathcal{A}[\psi](l) = 0$. The existence of $\mathcal{A}^{-1}$ yields $\psi(l) = 0$. Subsequently, $\{\Lambda_i(l)\}_{i=1}^{\infty}$ is complete on $\Pi(\mathcal{J})$. □

Definition 3. *[60] If ψ is a continuous function and $\left\{\overline{\Lambda}_i(l)\right\}_{i=1}^{\infty}$ an orthonormal functions system, then $\langle\psi(l),\overline{\Lambda}_i(l)\rangle_{\Pi}$, $i = 1,2,\dots$ are called Fourier functions of ψ with respect to the system $\left\{\overline{\Lambda}_i(l)\right\}_{i=1}^{\infty}$ and $\psi(l) = \sum_{i=1}^{\infty}\langle\psi(l),\overline{\Lambda}_i(l)\rangle_{\Pi}\overline{\Lambda}_i(l)$ is called its Fourier expansion.*

Theorem 3. *The subsequent are achieved:*

1. *Whenever $n \to \infty$ the analytic solution of (15) fulfills:*

$$\psi(l) = \sum_{i=1}^{\infty}\sum_{j=1}^{i}\varepsilon_{ij}\zeta\big(l_j,\psi\big(l_j\big),\partial_l\psi\big(l_j\big)\big)\overline{\Lambda}_i(l). \tag{32}$$

2. *The n-term numerical solution of Equation (15) fulfills:*

$$\psi^n(l) = \sum_{i=1}^{n}\sum_{j=1}^{i}\varepsilon_{ij}\zeta\big(l_j,\psi\big(l_j\big),\partial_l\psi\big(l_j\big)\big)\overline{\Lambda}_i(l). \tag{33}$$

Proof. Assume that ε_{ij} are orthogonalization coefficients for the orthonormal functions systems $\left\{\overline{\Lambda}_i(l)\right\}_{i=1}^{\infty}$. Then

$$\begin{aligned}\psi(l) &= \sum_{i=1}^{\infty}\langle\psi(l),\overline{\Lambda}_i(l)\rangle_{\Pi}\overline{\Lambda}_i(l)\\ &= \sum_{i=1}^{\infty}\left\langle\psi(l),\sum_{j=1}^{i}\varepsilon_{ij}\Lambda_j(l)\right\rangle_{\Pi}\overline{\Lambda}_i(l)\\ &= \sum_{i=1}^{\infty}\sum_{j=1}^{i}\varepsilon_{ij}\langle\psi(l),\mathcal{A}^*\big[\mathfrak{S}_j\big](l)\rangle_{\Pi}\overline{\Lambda}_i(l)\\ &= \sum_{i=1}^{\infty}\sum_{j=1}^{i}\varepsilon_{ij}\langle\mathcal{A}[\psi](l),\mathfrak{S}_j(l)\rangle_{\Delta}\,\overline{\Lambda}_i(l)\\ &= \sum_{i=1}^{\infty}\sum_{j=1}^{i}\varepsilon_{ij}\langle\zeta(l,\psi(l),\partial_l\psi(l)),\mathfrak{S}_j(l)\rangle_{\Delta}\,\overline{\Lambda}_i(l)\\ &= \sum_{i=1}^{\infty}\sum_{j=1}^{i}\varepsilon_{ij}\zeta\big(l_j,\psi\big(l_j\big),\partial_l\psi\big(l_j\big)\big)\overline{\Lambda}_i(l).\end{aligned} \tag{34}$$

For the numerical computations, we truncate the series in (32) using the n-term numerical solution of $\psi(l)$. □

The attached steps focusing on the computational steps require using an appropriate software package for solving (15) using RKDM, and in order to evaluate the numerical approximation ψ^n of ψ in $\Pi(\mathcal{J})$.

Algorithm 2. Steps of RKDM for numerical approximations model of FLETM in ABC derivative:

Step I: Fix l, k in $\mathcal{J}$ and do Phases 1 and 2:
- **Phase 1**: Set $l_i = \frac{1}{n} i$ in the index $i = 0, 1, \ldots, n$.
- **Phase 2:** Set $\Lambda_i(l) = \mathcal{A}^*[\mathfrak{S}_i](l)$ in the index $i = 1, 2, \ldots, n$.

Output: the orthogonal function system $\Lambda_i(l)$.
Step II: For the indices $i = 1, 2, \ldots$ and $j = 1, 2, \ldots, i-1$ do Algorithm 1.
Output: the orthogonalization coefficients ε_{ij}.
Step III: Set $\overline{\Lambda}_i(l) = \sum_{j=1}^{i} \varepsilon_{ij} \Lambda_j(l)$ in the indices $i = 1, 2, \ldots, n$.
Output: the orthonormal function system $\overline{\Lambda}_i(l)$.
Step IV: Set $\psi^0(l_1) = 0$ and with the indices $i = 1, 2, \ldots, n$ do Phases 1, 2, and 3:
- **Phase 1:** Set $\psi^i(l_i) = \psi^{i-1}(l_i)$.
- **Phase 2:** Set $\mathcal{F}_i = \sum_{j=1}^{i} \varepsilon_{ij} \zeta\big(l_j, \psi\big(l_j\big), \partial_l \psi\big(l_j\big)\big)$.
- **Phase 3:** Set $\psi^n(l) = \sum_{j=1}^{i} \mathcal{F}_j \overline{\Lambda}_j(l)$.

Output: The n-term numerical approximation $\psi^n(l)$ of $\psi(l)$.

---

4. Convergence Analysis

In this part, the convergence of numerical solution and error behavior are presented. Using convergent series representation, the following two theorems explain that FLETM described in Equation (15) is conditionally formulated and consistent.

To achieve our goal, we assume $\|\psi^{n-1}\|_\Pi$ is bounded whenever $n \to \infty$ and $\{l_i\}_{i=1}^{\infty}$ is dense on $\mathcal{J}$. Then the error $\mathcal{E}^n = \|\psi - \psi^n\|_\Pi^2$ is decreasing for sufficiently large n, since we have

$$\begin{aligned} \mathcal{E}^n - \mathcal{E}^{n-1} &= \| \sum_{i=n+1}^{\infty} \langle \psi(l), \overline{\Lambda}_i(l) \rangle_{\mathcal{A}} \overline{\Lambda}_i(l) \|_\Pi^2 - \| \sum_{i=n}^{\infty} \langle \mu(l), \overline{\Lambda}_i(l) \rangle_{\mathcal{A}} \overline{\Lambda}_i(l) \|_\Pi^2 \\ &= \sum_{i=n+1}^{\infty} \langle \psi(l), \overline{\Lambda}_i(l) \rangle_\Pi^2 - \sum_{i=n}^{\infty} \langle \psi(l), \overline{\Lambda}_i(l) \rangle_\Pi^2 \\ &< 0. \end{aligned} \tag{35}$$

The convergence of $\sum_{i=1}^{\infty} \langle \psi(l), \overline{\Lambda}_i(l) \rangle_\Pi \overline{\Lambda}_i(l)$ yields $\mathcal{E}^n \to 0$ whenever $n \to \infty$ as long as $\psi(l)$ and $\psi^n(l)$ are extracted from (32) and (33).

Lemma 2. *For $\psi \in \Pi(\mathcal{J})$, it holds $\big|\psi(l)\big| \le 3.5\|\psi\|_\Pi$, $\big|\partial_l \psi(l)\big| \le 3\|\psi\|_\Pi$, and $\big|\partial_l^2 \psi(l)\big| \le 2\|\psi\|_\Pi$.*

Proof. The proof is straightforward from $\partial_l^2 \psi(l) - \partial_l^2 \psi(0) = \int_0^l \partial_p^2 \psi(p) dp$, Holder's inequality, and (6). □

If $\|\psi^{n-1} - \psi\|_\Pi \to 0$ and $l_n \to k$ whenever $n \to \infty$ then $\zeta\big(l_n, \psi^{n-1}(l_n), \partial_l \psi^{n-1}(l_n)\big) \to \zeta(k, \psi(k), \partial_l \psi(k))$. This can be seen directly from Lemma 2 and the fact that $\zeta(l, \psi(l), \partial_l \psi(l)) \in C(\mathcal{J} \times \mathbb{R} \times \mathbb{R}, \mathbb{R})$. We denote $\mathcal{F}_i = \sum_{j=1}^{i} \varepsilon_{ij} \zeta\big(l_j, \psi\big(l_j\big), \partial_l \psi\big(l_j\big)\big)$. This allows us to rewrite $\psi^n(l)$ as

$$\psi^n(l) = \sum_{i=1}^{n} \mathcal{F}_i \overline{\Lambda}_i(l). \tag{36}$$

Theorem 4. *From (36), it holds that* $\psi^n(l) \to \psi(l)$ *whenever* $n \to \infty$.

Proof. Clearly, $\psi^{n+1}(l) = \psi^n(l) + \mathcal{F}_{n+1}\overline{\Lambda}_{n+1}(l)$. From the orthogonality of $\left\{\overline{\Lambda}_i(l)\right\}_{i=1}^{\infty}$, we get

$$\begin{aligned} \|\psi^{n+1}\|_{\Pi}^2 &= \|\psi^n\|_{\Pi}^2 + \mathcal{F}_{n+1}^2 \\ &= \|\psi^{n-1}\|_{\Pi}^2 + \mathcal{F}_n^2 + \mathcal{F}_{n+1}^2 \\ &= \dots \\ &= \|\psi^0\|_{\Pi}^2 + \sum_{i=1}^{n+1} \mathcal{F}_i^2. \end{aligned} \tag{37}$$

This implies $\|\psi^{n+1}\|_{\Pi} \geq \|\psi^n\|_{\Pi}$ and there exists γ in $\mathbb{R}$ such that $\sum_{i=1}^{\infty} \mathcal{F}_i^2 = \gamma$, which means that $\left\{\mathcal{F}_i^2\right\}_{i=1}^{\infty} \in l^2$. In order to have

$$\psi^m(l) - \psi^{m-1}(l) \perp \psi^{m-1}(l) - \psi^{m-2}(l) \perp \dots \perp \psi^{n+1}(l) - \psi^n(l), \tag{38}$$

it is sufficient to have for $m > n$ that

$$\begin{aligned} \|\psi^m - \psi^n\|_{\Pi}^2 &= \|\psi^m - \psi^{m-1} + \psi^{m-1} - \dots + \psi^{n+1} - \psi^n\|_{\Pi}^2 \\ &= \|\psi^m - \psi^{m-1}\|_{\Pi}^2 + \|\psi^{m-1} - \psi^{m-2}\|_{\Pi}^2 + \dots + \|\psi^{n+1} - \psi^n\|_{\Pi}^2, \end{aligned} \tag{39}$$

whereas, $\|\psi^m - \psi^{m-1}\|_{\Pi}^2 = \mathcal{F}_m^2$. As $n, m \to \infty$ one has $\|\psi^m - \psi^n\|_{\Pi}^2 = \sum_{l=n+1}^{m} \mathcal{F}_i^2 \to 0$. By the completeness, $\exists \psi^n(l) \in \Pi(\mathcal{J})$ such that $\psi^n(l) \to \psi(l)$ as $n \to \infty$. □

Theorem 5. *One has* $\psi(l) = \sum_{i=1}^{\infty} \mathcal{F}_i \overline{\Lambda}_i(l)$ *whenever* $n \to \infty$ *in (36).*

Proof. Taking the $\lim\limits_{n\to\infty}$ on both sides of (36), one get $\psi(l) = \sum_{i=1}^{\infty} \mathcal{F}_i \overline{\Lambda}_i(l)$. Thus

$$\begin{aligned} \mathcal{A}[\psi](l_k) &= \sum_{i=1}^{\infty} \mathcal{F}_i \langle \mathcal{A}\left[\overline{\Lambda}_i\right](l), \mathfrak{S}_k(l) \rangle_{\Delta} \\ &= \sum_{i=1}^{\infty} \mathcal{F}_i \langle\, \overline{\Lambda}_i(l), \mathcal{A}^*[\mathfrak{S}_k](l) \rangle_{\Pi} \\ &= \sum_{i=1}^{\infty} \mathcal{F}_i \langle \overline{\Lambda}_i(l), \Lambda_k(l) \rangle_{\Pi}, \end{aligned} \tag{40}$$

and

$$\begin{aligned} \sum_{k'=1}^{l} \varepsilon_{kk'} \mathcal{A}[\psi](l_{k'}) &= \sum_{i=1}^{\infty} \mathcal{F}_i \langle \overline{\Lambda}_i(l), \sum_{k'=1}^{l} \varepsilon_{kk'} \Lambda_{k'}(l) \rangle_{\Pi} \\ &= \sum_{i=1}^{\infty} \mathcal{F}_i \langle \overline{\Lambda}_i(t), \overline{\Lambda}_{k'}(l) \rangle_{\Pi} \\ &= \mathcal{F}_l. \end{aligned} \tag{41}$$

If $l = 1$, then $\mathcal{A}[\psi](l_1) = \zeta\left(l_1, \psi^0(l_1), \partial_l \psi^0(l_1)\right)$ and if $l = 2$, then $\mathcal{A}[\psi](l_2) = \zeta\left(l_2, \psi^1(l_2), \partial_l \psi^1(l_2)\right)$. Generally, we have $\mathcal{A}[\psi](l_n) = \zeta\left(l_n, \psi^{n-1}(l_n), \partial_l \psi^{n-1}(l_n)\right)$. By the density condition, $\forall k \in \mathcal{J}$; $\exists \left\{l_{n_q}\right\}_{q=1}^{\infty}$ such that $l_{n_q} \to k$ whenever $q \to \infty$ or $\mathcal{A}[\psi]\left(l_{n_q}\right) = \zeta\left(l_{n_q}, \psi^{n_q-1}\left(l_{n_q}\right), \partial_l \psi^{n_q-1}\left(l_{n_q}\right)\right)$. Letting $j \to \infty$ one can get $\mathcal{A}[\psi](k) = \zeta(k, \psi(k), \partial_l \psi(k))$. Since $\overline{\Lambda}_i(l) \in \Pi(\mathcal{J})$, then $\psi(l)$ satisfies (15). □

5. Model Experiments and Computational Results

In this important portion; in order to solve FLETM in (1) and (2) numerically using the RKDM, three models are presented in certain specific form. In the examples, we demonstrate the performance and efficiency of the proposed approach in term of tables and figures, with some scientific explanations' comments.

5.1. Certain Examples

In the subsequent FLETM, the readers should note that $\psi(0)$ and $\partial_l\psi(0)$ are known and may not be homogeneous. The forcing term $\mathrm{T}(l)$ can be obtain by substituting $\psi(l)$ through the given model.

Example 1. *Consider the following FLETM in ABC sense:*

$$ {}_0^{ABC}\partial_l^\delta\psi(l) + \frac{1}{l}\partial_l\psi(l) + \frac{1}{l}\psi(l) + ln(\psi(l)) = \mathrm{T}(l), \tag{42}$$

subject to the CICs

$$\psi(0) = 1 \text{ and } \partial_l\psi(0) = \delta, \tag{43}$$

where the analytic solution is given by

$$\psi(l) = e^{\delta l}. \tag{44}$$

Example 2. *Consider the following FLETM in ABC sense:*

$$ {}_0^{ABC}\partial_l^\delta\psi(l) + \frac{1}{sin(l)}\partial_l\psi(l) - \psi(l) + sin(\psi(l)) = \mathrm{T}(l), \tag{45}$$

subject to the CICs

$$\psi(0) = 0 \text{ and } \partial_l\psi(0) = 0, \tag{46}$$

where the analytic solution is given by

$$\psi(l) = l^{2\delta} - l^3. \tag{47}$$

Example 3. *Consider the following FLETM in ABC sense:*

$$ {}_0^{ABC}\partial_l^\delta\psi(l) + \frac{1}{l^2}\partial_l\psi(l) - \frac{1}{l^4}\psi(l) + \sqrt[3]{\psi(l)} = \mathrm{T}(l), \tag{48}$$

subject to the CICs

$$\psi(0) = 0 \text{ and } \partial_l\psi(0) = \delta, \tag{49}$$

where the analytic solution is given by

$$\psi(l) = \delta l - l^2. \tag{50}$$

Recall that $l \in [0,1]$; $\delta \in (1,2]$; $\psi \in C(\mathcal{J} \to \mathbb{R})$; and $\mathrm{T} \in C(\mathcal{J} - \{0\} \to \mathbb{R})$, while ${}_0^{ABC}\partial_l^\delta\psi(l)$ denotes the ABC fractional derivative of ψ in l over $\mathcal{J}$ of order δ.

5.2. Results and Discussions

Take into consideration Algorithms 1 and 2, following the RKDM, using $l_i = \frac{i}{n}, i = 0, 1, \ldots, n = 50$ the numerical validations for different values of grid points $l_i \in \mathcal{J}$ will be exhibited. For this purpose, Tables 1–3 tabulates the evolution of the absolute errors Ab as

$$Ab\left[\psi^{50}\right](l_i) = \left|\psi(l_i) - \psi^{50}(l_i)\right|, \tag{51}$$

for Examples 1, 2, and 3, simultaneously.

Table 1. Numerical results of Example 1 using RKDM.

	δ=2	δ=1.75	δ=1.5	δ=1.25
l_i	$Ab[\psi^{50}](l_i)$	$Ab[\psi^{50}](l_i)$	$Ab[\psi^{50}](l_i)$	$Ab[\psi^{50}](l_i)$
0	0	0	0	0
0.1	5.58923×10^{-7}	2.39589×10^{-6}	9.76028×10^{-6}	1.26481×10^{-5}
0.2	7.29487×10^{-7}	8.43183×10^{-6}	5.53946×10^{-5}	4.51370×10^{-4}
0.3	5.10731×10^{-7}	9.31378×10^{-6}	6.44253×10^{-5}	8.45264×10^{-4}
0.4	4.86899×10^{-7}	4.02242×10^{-6}	5.96694×10^{-5}	6.39510×10^{-4}
0.5	3.73586×10^{-7}	6.44048×10^{-6}	9.76767×10^{-5}	8.49810×10^{-4}
0.6	5.96425×10^{-7}	9.83946×10^{-6}	3.13543×10^{-5}	7.18295×10^{-4}
0.7	8.30602×10^{-7}	8.11052×10^{-6}	1.78901×10^{-5}	2.28708×10^{-4}
0.8	3.09230×10^{-7}	3.03588×10^{-6}	8.12647×10^{-5}	5.51276×10^{-4}
0.9	7.82026×10^{-6}	2.81165×10^{-6}	5.67583×10^{-5}	6.57153×10^{-4}
1.0	6.27080×10^{-6}	3.20502×10^{-5}	2.14565×10^{-4}	3.76831×10^{-4}

Table 2. Numerical results of Example 2 using RKDM.

	δ=2	δ=1.75	δ=1.5	δ=1.25
l_i	$Ab[\psi^{50}](l_i)$	$Ab[\psi^{50}](l_i)$	$Ab[\psi^{50}](l_i)$	$Ab[\psi^{50}](l_i)$
0	0	0	0	0
0.1	1.66034×10^{-7}	3.79764×10^{-6}	8.68106×10^{-5}	7.78427×10^{-4}
0.2	2.58021×10^{-7}	6.04130×10^{-6}	6.66813×10^{-5}	4.83384×10^{-4}
0.3	2.47746×10^{-7}	2.43097×10^{-6}	5.42359×10^{-5}	4.13100×10^{-4}
0.4	6.83007×10^{-8}	7.36473×10^{-6}	1.28745×10^{-5}	9.26837×10^{-4}
0.5	1.54628×10^{-7}	7.49228×10^{-6}	7.24921×10^{-5}	2.34712×10^{-4}
0.6	4.61756×10^{-7}	9.86819×10^{-6}	3.86754×10^{-5}	7.72225×10^{-4}
0.7	8.34165×10^{-8}	6.41801×10^{-6}	2.32842×10^{-5}	2.55304×10^{-4}
0.8	9.75666×10^{-8}	6.05864×10^{-6}	6.41085×10^{-5}	5.48677×10^{-4}
0.9	1.96125×10^{-7}	1.54146×10^{-6}	5.49951×10^{-5}	6.03551×10^{-4}
1.0	2.45293×10^{-7}	9.86166×10^{-6}	2.78153×10^{-5}	9.96146×10^{-4}

Table 3. Numerical results of Example 3 using RKDM.

	δ=2	δ=1.75	δ=1.5	δ=1.25
l_i	$Ab[\psi^{50}](l_i)$	$Ab[\psi^{50}](l_i)$	$Ab[\psi^{50}](l_i)$	$Ab[\psi^{50}](l_i)$
0	0	0	0	0
0.1	8.72538×10^{-7}	8.35309×10^{-6}	4.24210×10^{-5}	9.37424×10^{-4}
0.2	7.62576×10^{-7}	5.90241×10^{-6}	1.89126×10^{-5}	4.86929×10^{-4}
0.3	4.31937×10^{-7}	7.87242×10^{-6}	9.13479×10^{-5}	2.67124×10^{-4}
0.4	4.71124×10^{-7}	3.19969×10^{-6}	7.50933×10^{-5}	7.64597×10^{-4}
0.5	3.51107×10^{-6}	6.03111×10^{-6}	4.86751×10^{-5}	7.01821×10^{-4}
0.6	8.69821×10^{-6}	6.45966×10^{-5}	2.98386×10^{-5}	8.42708×10^{-4}
0.7	2.50806×10^{-6}	2.80152×10^{-5}	7.89215×10^{-5}	4.27468×10^{-4}
0.8	1.25974×10^{-6}	3.66312×10^{-5}	4.03998×10^{-5}	8.68758×10^{-4}
0.9	2.14535×10^{-6}	5.01585×10^{-5}	1.76836×10^{-4}	8.38715×10^{-4}
1.0	2.93206×10^{-6}	1.57354×10^{-5}	2.81862×10^{-4}	9.03151×10^{-4}

From the tables, we observe that the RKDM numerical outcomes are unanimous with analytic solutions during in the area of interest. Additional iterations will lead to more refined solutions along the memory and heritage characteristics of δ. The ABC fractional derivative orders have powerful belongings on the model shapes, which head for lead to remarkable behaviors in the incident of a considerable departure from the value of $\delta = 2$.

The $3D$ surfaces plot of the RKDM numerical solutions for Examples 1, 2, and 3 are drawn in Figure 1a–c simultaneously, for different values of grid points $l_i \in \mathcal{J}$ when $\delta \in (1, 2]$. It appears that all figures almost look identical in their behaviors, and in good agreement with each other, particularly when comparing the case of $\delta = 2$. Moreover, the RKDM numerical solutions are very close at the CICs.

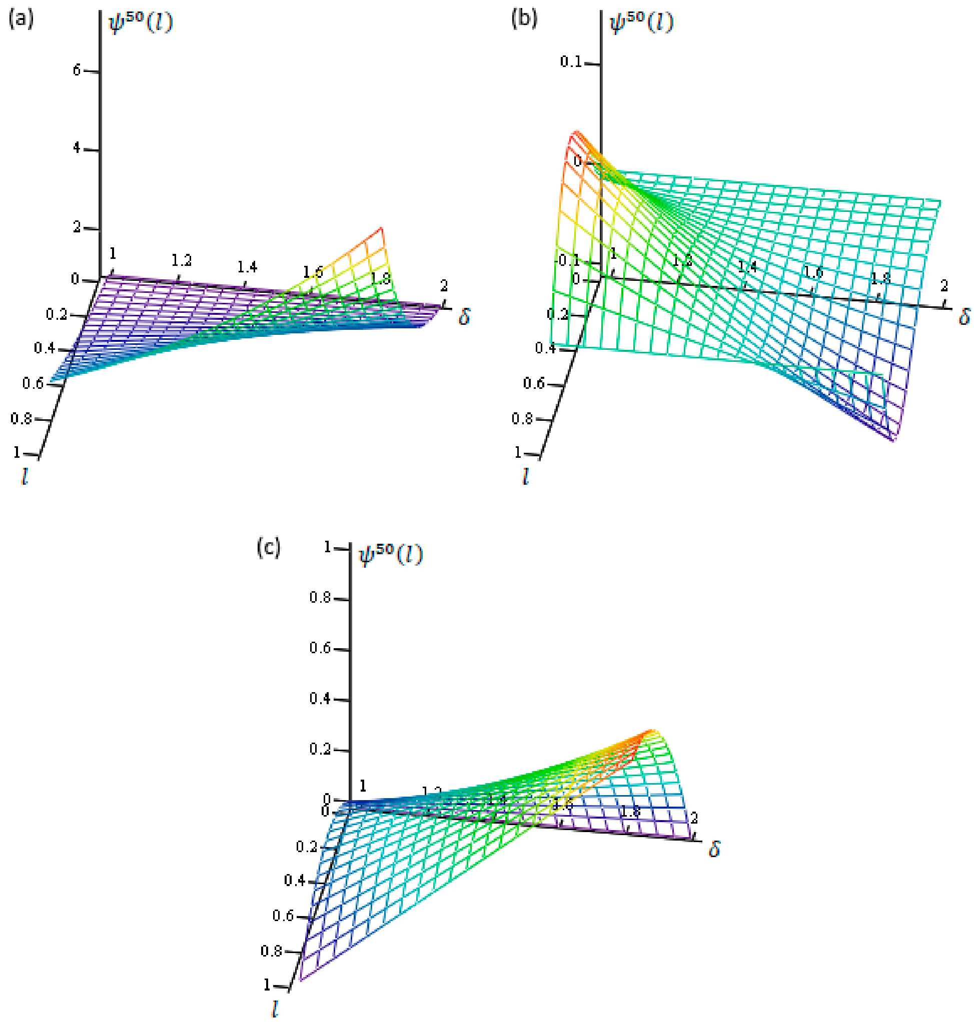

Figure 1. The 3*D* computational values of the RKDM when $l_i \in \mathcal{J}$ and $\delta \in (1,2]$: (**a**) Example 1; (**b**) Example 2; and (**c**) Example 3.

6. Conclusions and Outline

The attractive RKDM has been successfully employed to construct and predict the numerical/analytic solutions for FLETM under the ABC fractional sense. Convergence and consistency were discussed, which turns out that the proposed scheme has decreasing absolute error in the $\Pi(\mathcal{J})$ space. Three FLETM models have been given to test applicability and straightforwardness of the presented approach. The gained numerical data reveal that the numerical solutions are conformable with each other at the selected parameters and nods. Finally, one can see that the RKDM is a methodical and convenient scheme to address various fractional differential/integral problems across applied sciences and engineering area.

In the near future, we intend to conduct more research as a continuation of this work. One of these research studies is related to the applications of the RKDM to solve numerically the Lane–Emden type models that contain functions with singularities or weak regularity, subject to CICs or constraint boundary conditions.

Author Contributions: Conceptualization, O.A.A. and S.M.; methodology O.A.A.; software, A.-H.A.-A.; validation, M.S.O. and A.-B.A.M.; formal analysis, O.A.A.; investigation, O.A.A.; resources, M.S.O.; data curation, A.-H.A.-A.; writing—original draft preparation, M.S.O.; writing—review and editing, O.A.A.; visualization, O.A.A.; supervision, S.M.; project administration, A.-B.A.M.; funding acquisition, A.-B.A.M. All authors have read and agreed to the published version of the manuscript.

Funding: This project was supported by the Deanship of Scientific Research at Prince Sattam Bin Abdulaziz University under the research project No.2020/01/11801.

Acknowledgments: This research was supported by the Ajman University grant: 2019–20.

Conflicts of Interest: The authors declare no conflict of interest.

Abbreviations

FLETM	fractional Lane–Emden type model
ABC	Atangana–Baleanu–Caputo
RKDM	reproducing kernel discretization method
CIC	constraint initial condition

References

1. Herrmann, R. *Fractional Calculus: An Introduction for Physicists*; World Scientific: Singapore, 2014.
2. Tarasov, V.E. *Fractional Dynamics: Applications of Fractional Calculus to Dynamics of Particles, Fields and Media*; Springer: Heidelberg, Germany, 2011.
3. West, B.J. *Fractional Calculus View of Complexity: Tomorrow's Science*; Taylor & Francis: Oxfordshire, UK, 2015.
4. Kilbas, A.; Srivastava, H.; Trujillo, J. *Theory and Applications of Fractional Differential Equations*; Elsevier: Amsterdam, The Netherlands, 2006.
5. West, B.J. *Natures Patterns and the Fractional Calculus*; De Gruyter: Berlin, Germany, 2017.
6. Abu Arqub, O.; El-Ajou, A.; Momani, S. Constructing and predicting solitary pattern solutions for nonlinear time-fractional dispersive partial differential equations. *J. Comput. Phys.* **2015**, *293*, 385–399. [CrossRef]
7. El-Ajou, A.; Abu Arqub, O.; Momani, S. Approximate analytical solution of the nonlinear fractional KdV-Burgers equation: A new iterative algorithm. *J. Comput. Phys.* **2015**, *293*, 81–95. [CrossRef]
8. El-Ajou, A.; Abu Arqub, O.; Momani, S.; Baleanu, D.; Alsaedi, A. A novel expansion iterative method for solving linear partial differential equations of fractional order. *Appl. Math. Comput.* **2015**, *257*, 119–133. [CrossRef]
9. Ray, S.S. New exact solutions of nonlinear fractional acoustic wave equations in ultrasound. *Comput. Math. Appl.* **2016**, *71*, 859–868.
10. Ray, S.S.; Sahoo, S. Analytical approximate solutions of Riesz fractional diffusion equation and Riesz fractional advection-dispersion equation involving nonlocal space fractional derivatives. *Math. Method. Appl. Sci.* **2015**, *38*, 2840–2849. [CrossRef]
11. Ghanbari, B.; Osman, M.S.; Baleanu, D. Generalized exponential rational function method for extended Zakharov–Kuzetsov equation with conformable derivative. *Mod. Phys. Lett. A* **2019**, *34*, 1950155. [CrossRef]
12. Zhuang, P.; Liu, F.; Anh, V.; Turner, I. Numerical methods for the variable-order fractional advection-diffusion equation with a nonlinear source term. *SIAM J. Numer. Anal.* **2009**, *47*, 1760–1781. [CrossRef]
13. Osman, M.S. New analytical study of water waves described by coupled fractional variant Boussinesq equation in fluid dynamics. *Pramana* **2019**, *93*, 26. [CrossRef]
14. Liu, J.G.; Osman, M.S.; Zhu, W.H.; Zhou, L.; Ai, G.P. Different complex wave structures described by the Hirota equation with variable coefficients in inhomogeneous optical fibers. *Appl. Phys. B* **2019**, *125*, 175. [CrossRef]
15. Osman, M.S.; Wazwaz, A.M. A general bilinear form to generate different wave structures of solitons for a (3+ 1) -dimensional Boiti-Leon-Manna-Pempinelli equation. *Math. Method Appl. Sci.* **2019**, *42*, 6277–6283. [CrossRef]
16. Osman, M.S.; Lu, D.; Khater, M.M.A.; Attia, R.A.M. Complex wave structures for abundant solutions related to the complex Ginzburg–Landau model. *Optik* **2019**, *192*, 162927. [CrossRef]
17. Ding, Y.; Osman, M.S.; Wazwaz, A.M. Abundant complex wave solutions for the nonautonomous Fokas–Lenells equation in presence of perturbation terms. *Optik* **2019**, *181*, 503–513. [CrossRef]
18. Lu, D.; Tariq, K.U.; Osman, M.S.; Baleanu, D.; Younis, M.; Khatera, M.M.A. New analytical wave structures for the (3 + 1)-dimensional Kadomtsev-Petviashvili and the generalized Boussinesq models and their applications. *Results Phys.* **2019**, *14*, 102491. [CrossRef]
19. Atangana, A.; Baleanu, D. New fractional derivatives with non-local and non-singular kernel: Theory and application to heat transfer model. *Therm. Sci.* **2016**, *20*, 763–769. [CrossRef]

20. Atangana, A.; Nieto, J.J. Numerical solution for the model of RLC circuit via the fractional derivative without singular kernel. *Adv. Mech. Eng.* **2015**, *7*, 1–7. [CrossRef]
21. Maayah, B.; Yousef, F.; Abu Arqub, O.; Momani, S.; Alsaedi, A. Computing bifurcations behavior of mixed type singular time-fractional partial integrodifferential equations of Dirichlet functions types in Hilbert space with error analysis. *Filomat* **2019**, *33*, 3845–3853. [CrossRef]
22. Atangana, A.; Gómez-Aguilar, J.F. Decolonisation of fractional calculus rules: Breaking commutativity and associativity to capture more natural phenomena. *Eur. Phys. J. Plus* **2018**, *133*, 1–22. [CrossRef]
23. Abu Arqub, O.; Al-Smadi, M. Atangana-Baleanu fractional approach to the solutions of Bagley-Torvik and Painlevé equations in Hilbert space. *Chaos Solitons Fractals* **2018**, *117*, 161–167. [CrossRef]
24. Abu Arqub, O.; Maayah, B. Modulation of reproducing kernel Hilbert space method for numerical solutions of Riccati and Bernoulli equations in the Atangana-Baleanu fractional sense. *Chaos Solitons Fractals* **2019**, *125*, 163–170. [CrossRef]
25. Abu Arqub, O.; Maayah, B. Numerical solutions of integrodifferential equations of Fredholm operator type in the sense of the Atangana-Baleanu fractional operator. *Chaos Solitons Fractals* **2018**, *117*, 117–124. [CrossRef]
26. Abu Arqub, O.; Maayah, B. Fitted fractional reproducing kernel algorithm for the numerical solutions of ABC-Fractional Volterra integro-differential equations. *Chaos Solitons Fractals* **2019**, *126*, 394–402. [CrossRef]
27. Djida, J.D.; Atangana, A.; Area, I. Numerical computation of a fractional derivative with non-local and non-singular kernel. *Math. Model. Nat. Phenom.* **2017**, *12*, 4–13. [CrossRef]
28. Atangana, A.; Gómez-Aguilar, J.F. Fractional derivatives with no-index law property: Application to chaos and statistic. *Chaos Solitons Fractals* **2018**, *114*, 516–535. [CrossRef]
29. Atangana, A. On the new fractional derivative and application to nonlinear Fisher′s reaction-diffusion equation. *Appl. Math. Comput.* **2016**, *273*, 948–956. [CrossRef]
30. Atangana, A.; Koca, I. On the new fractional derivative and application to Nonlinear Baggs and Freedman model. *J. Nonlinear Sci. Appl.* **2016**, *9*, 2467–2480. [CrossRef]
31. Algahtani, O. Comparing the Atangana-Baleanu and Caputo-Fabrizio derivative with fractional order: Allen Cahn model. *Chaos Solitons Fractals* **2016**, *89*, 552–559. [CrossRef]
32. Akgül, A.; Inc, M.; Karatas, E.; Baleanu, D. Numerical solutions of fractional differential equations of Lane-Emden type by an accurate technique. *Adv. Differ. Equ.* **2015**, *2015*, 220. [CrossRef]
33. Singh, O.P.; Pandey, R.K.; Singh, V.K. An analytic algorithm of Lane–Emden type equations arising in astrophysics using modified Homotopy analysis method. *Comput. Phys. Commun.* **2009**, *180*, 1116–1124. [CrossRef]
34. Kıymaz, O.; Mirasyedioğlu, Ş. A new symbolic computational approach to singular initial value problems in the second-order ordinary differential equation. *Appl. Math. Comput.* **2005**, *171*, 1218–1225.
35. Iqbal, S.; Javed, A. Application of optimal homotopy asymptotic method for the analytic solution of singular Lane–Emden type equation. *Appl. Math. Comput.* **2011**, *217*, 7753–7761. [CrossRef]
36. Pandey, R.K.; Kumar, N. Solution of Lane–Emden type equations using Bernstein operational matrix of differentiation. *New Astron.* **2012**, *17*, 303–308. [CrossRef]
37. Cui, M.; Lin, Y. *Nonlinear Numerical Analysis in the Reproducing Kernel Space*; Nova Science: Hauppauge, NY, USA, 2009.
38. Berlinet, A.; Agnan, C.T. *Reproducing Kernel Hilbert Space in Probability and Statistic*; Kluwer Academic Publishers: New York, NY, USA, 2004.
39. Daniel, A. *Reproducing Kernel Spaces and Applications*; Springer: Basel, Switzerland, 2003.
40. Abu Arqub, O.; Al-Smadi, M.; Momani, S.; Hayat, T. Numerical solutions of fuzzy differential equations using reproducing kernel Hilbert space method. *Soft Comput.* **2016**, *20*, 3283–3302. [CrossRef]
41. Abu Arqub, O.; Al-Smadi, M.; Momani, S.; Hayat, T. Application of reproducing kernel algorithm for solving second-order, two-point fuzzy boundary value problems. *Soft Comput.* **2017**, *21*, 7191–7206. [CrossRef]
42. Abu Arqub, O. Adaptation of reproducing kernel algorithm for solving fuzzy Fredholm-Volterra integrodifferential equations. *Neural Comput. Appl.* **2017**, *28*, 1591–1610. [CrossRef]
43. Abu Arqub, O. Fitted reproducing kernel Hilbert space method for the solutions of some certain classes of time-fractional partial differential equations subject to initial and Neumann boundary conditions. *Comput. Math. Appl.* **2017**, *73*, 1243–1261. [CrossRef]
44. Abu Arqub, O. Numerical solutions for the Robin time-fractional partial differential equations of heat and fluid flows based on the reproducing kernel algorithm. *Int. J. Numer. Meth. Heat* **2018**, *28*, 828–856. [CrossRef]

45. Abu Arqub, O. The reproducing kernel algorithm for handling differential algebraic systems of ordinary differential equations. *Math. Meth. Appl. Sci.* **2016**, *39*, 4549–4562. [CrossRef]
46. Abu Arqub, O.; Al-Smadi, M.; Shawagfeh, N. Solving Fredholm integro-differential equations using reproducing kernel Hilbert space method. *Appl. Math. Comput.* **2013**, *219*, 8938–8948. [CrossRef]
47. Abu Arqub, O.; Al-Smadi, M. Numerical algorithm for solving two-point, second-order periodic boundary value problems for mixed integro-differential equations. *Appl. Math. Comput.* **2014**, *243*, 911–922. [CrossRef]
48. Abu Arqub, O. Approximate solutions of DASs with nonclassical boundary conditions using novel reproducing kernel algorithm. *Fundam. Inform.* **2016**, *146*, 231–254. [CrossRef]
49. Abu Arqub, O.; Al-Smadi, M. Numerical algorithm for solving time-fractional partial integrodifferential equations subject to initial and Dirichlet boundary conditions. *Numer. Meth. Part. Differ. Equ.* **2018**, *34*, 1577–1597. [CrossRef]
50. Abu Arqub, O. Solutions of time-fractional Tricomi and Keldysh equations of Dirichlet functions types in Hilbert space. *Numer. Meth. Part. Differ. Equ.* **2018**, *34*, 1759–1780. [CrossRef]
51. Abu Arqub, O. Numerical solutions of systems of first-order, two-point BVPs based on the reproducing kernel algorithm. *Calcolo* **2018**, *55*, 1–28. [CrossRef]
52. Abu Arqub, O.; Odibat, Z.; Al-Smadi, M. Numerical solutions of time-fractional partial integrodifferential equations of Robin functions types in Hilbert space with error bounds and error estimates. *Nonlinear Dyn.* **2018**, *94*, 1819–1834. [CrossRef]
53. Abu Arqub, O.; Al-Smadi, M. An adaptive numerical approach for the solutions of fractional advection–diffusion and dispersion equations in singular case under Riesz's derivative operator. *Physica A* **2020**, *540*, 123257. [CrossRef]
54. Abu Arqub, O. Numerical algorithm for the solutions of fractional order systems of Dirichlet function types with comparative analysis. *Fundam. Inform.* **2019**, *166*, 111–137. [CrossRef]
55. Al-Smadi, M.; Abu Arqub, O. Computational algorithm for solving fredholm time-fractional partial integrodifferential equations of dirichlet functions type with error estimates. *Appl. Math. Comput.* **2019**, *342*, 280–294. [CrossRef]
56. Abu Arqub, O.; Shawagfeh, N. Application of reproducing kernel algorithm for solving Dirichlet time-fractional diffusion-Gordon types equations in porous media. *J. Porous Media* **2019**, *22*, 411–434. [CrossRef]
57. Jiang, W.; Chen, Z. A collocation method based on reproducing kernel for a modified anomalous sub-diffusion equation. *Numer. Meth. Part. Differ. Equ.* **2014**, *30*, 289–300. [CrossRef]
58. Geng, F.Z.; Qian, S.P.; Li, S. A numerical method for singularly perturbed turning point problems with an interior layer. *J. Comput. Appl. Math.* **2014**, *255*, 97–105. [CrossRef]
59. Lin, Y.; Cui, M.; Yang, L. Representation of the exact solution for a kind of nonlinear partial differential equations. *Appl. Math. Lett.* **2006**, *19*, 808–813. [CrossRef]
60. Parashar, B.P. *Differential and Integral Equations*, 2nd ed.; CBS Publishers: Delhi, India, 2008.